Supporting Information

Oxidative Stabilization of Dilute Ether Electrolytes via Anion Modification

John Holoubek[a], Qizhang Yan[a], Haodong Liu[a], Emma J. Hopkins[b], Zhaohui Wu[c], Sicen Yu[b], Jian Luo[a,b,c,d], Tod A. Pascal[a,c,d], Zheng Chen [a,b,c,d], Ping Liu[a,b,c,d,*]

[a]*Department of NanoEngineering, University of California, San Diego, La Jolla, CA 92093, USA*

[b]*Program of Materials Science, University of California, San Diego, La Jolla, CA 92093, USA*

[c]*Program of Chemical Engineering, University of California, San Diego, La Jolla, CA 92093, USA*

[d]*Sustainable Power and Energy Center, University of California, San Diego, La Jolla, CA 92093, USA*

Materials and Methods

Anhydrous 1,2-dimethoxyethane (99.5%, DME) was purchased from Sigma Aldrich and used as received. Lithium bis(trifluoro methanesulfonyl)imide (LiTFSI), lithium trifluoromethanesulfonate (LiOTF), lithium bis(nonafluorobutanesulfonyl)imide (LiNFSI) and lithium nonafluorobutanesulfonate (LiNFS) was purchased from TCI and used as received. All electrolyte materials were stored in an Ar filled glovebox kept at < 0.5 ppm O_2 and < 0.1 ppm H_2O, where they were kept until the electrolytes were prepared and employed in coin cells. The electrolytes were prepared by adding predetermined amounts of lithium salt (1 mol/L) into DME followed by stirring until a clear solution was obtained. $LiNi_{0.8}Co_{0.2}Mn_{0.2}O_2$ (NMC 811) was purchased from Targray. NMC 811 electrodes for cycling tests were prepared by mixing the NMC 811 powder, Super-P and PVDF (KYNAR 2800) in a ratio of 96:2:2 or 80:10:10 dispersed in N-methyl pyrrolidinone (NMP, Sigma) solvent in sealed containers in a Thinky orbital mixer. The NMC 811 powder was added to the electrode slurries under Ar to minimize water and oxygen contact. After mixing the slurries were cast on Al foil (MTI) and dried in a vacuum oven at 120 °C overnight, and calendared in a mechanical roller. The final active mass loading for the NMC 811 electrodes were ~ 5 mg cm^{-2}. For XPS tests, NMC 811 electrodes were prepared using NMC 811, Super P, and PAN (80:10:10 by mass) dispersed in n-dimethylformamide in an otherwise identical process.

All coin cells were assembled in an Ar filled glovebox kept at < 0.5 ppm O_2 and < 0.1 ppm H_2O. For electrochemical tests Al-clad CR-2032 type coin cells (purchased from MTI) were assembled with prepared cathodes and counter electrodes separated by a 25 μm Celgard membrane soaked with 75 μL of electrolyte. For half cell cycling tests, 250 μm Li metal chips were purchased from Xiamen TOB New Energy Technology Co. LTD. and paired with the NMC 811 electrodes. Linear scan voltammetry (LSV) and potentiostatic stability tests were conducted with 250 μm Li and a blocking working electrode made of Al foil or 306-stainless steel.

Characterization

The ex-situ electrode samples were obtained from coin cells and washed with DME before analysis. XPS (Kratos Analytical, Kratos AXIS Supra) was carried out using Al anode source at 15 kV and all the peaks were fitted based on the reference C-C bond at 284.6 eV. All XPS measurements were collected with a 300 mm × 700 mm spot size during acquisition. Survey scans

were collected with a 1.0 eV step size, and were followed by high resolution scans with a step size of 0.05 eV for C 1s, O 1s, F 1s, and S2p regions. All prepared samples were placed in a heat-sealed bag inside the glovebox before they were transferred to the XPS.

Cryo-TEM characterization was conducted using a JEOL 2800 TEM at 200 kV with a Gatan 626 single tilt cooling holder. The sample temperature was maintained at about -170 oC to minimize the TEM beam damage on CEI morphology. For TEM sample preparation, the cycled cathode material was gently removed from the current collector with tweezer in an Ar-filled glovebox. Lacey carbon on 200 mesh Cu TEM grid was used to collect the powder and sealed in an Al-laminated pouch bag. During the TEM sample loading, a gentle Ar flow was maintained near the sample holder to minimize the air exposure. The cycled electrodes powders were first scraped off of the electrodes with a razor blade, followed by mechanical hand milling in an Ar atmosphere to reduce the particle size. Afterwards, the powders were placed onto a Ted Pella carbon coated Cu TEM grid. The TEM grid was placed in a membrane box and sealed in an aluminum laminated film pouch. During sample transfer to the TEM, direct Ar flow was applied toward the sample holder to minimize air exposure. The Digital Micrograph software was used to perform the EDS data processing.

Electrochemical Testing

All electrochemical data provided in this work were produced by CR-2032 type coin cells assembled in an Ar filled glovebox kept at < 0.5 ppm O_2 and < 0.1 ppm H_2O. All galvanostatic testing was done on Newware BTS 4000 or Arbin LBT-10V5A systems and all potentiostatic tests were carried out on a Biologic VSP-300 potentiostat. Half cell cycling consisted of 2 conditioning cycles at C/10 followed by C/3 indefinitely for both charge and discharge. The specific capacity basis for C rate determination was 200 mAh g^{-1} with respect to the cathode. The oxidative stability of the electrolytes was determined via LSV of a Li||Al or Li||SS cell at 1 mV s^{-1}, or a potentiostatic hold at the described potential of interest for 1 hr. Li||Cu coulombic efficiency measurements were carried out using the accurate method proposed by Adams *et al*.[1]

MD Simulations

Molecular Dynamics (MD) simulations were performed in LAMMPS using the OPLS-AA forcefield[2] for solvents and Li^+ with the anion description from Gaouveia et al.[3] For electrolyte structure determination, simulation boxes containing 20 salt and 255 DME molecules (corresponding to 1 mol/L) were constructed (Table S1). In all cases the charges of the Li^+ and FSI^- molecules were scaled to the high-frequency dielectric properties of the solvents present in the system according to the method employed by Park *et al*.[4] which is 0.73 for DME.

For each system, an initial energy minimization at 0 K (energy and force tolerances of 10^{-4}) was performed to obtain the ground-state structure. After this, the system was slowly heated from 0 K to room temperature at constant volume over 0.01 ns using a Langevin thermostat, with a damping parameter of 100 ps. The system was then subjected to 5 cycles of quench-annealing dynamics in order to eliminate the persistence of any meta-stable states, where the temperature was slowly cycled between 298 K and 894 with a ramp period 0.025 ns followed by 0.1 ns of dynamics at either temperature extreme. All 5 anneal cycles thus take 1.25 ns total. After annealing, the system was equilibrated in the constant temperature (298 K), constant pressure (1bar) (NpT ensemble) for 1.5 ns. We resolved stresses in the system isotropically using the Andersen barostat (pressure relaxation constant of 1 ps). We used the Shinoda et al.[5] equations

of motion which combine the hydrostatic equations of Martyna et al.[6] with the strain energy proposed by Parrinello and Rahman[7]. The time integration schemes closely follow the time-reversible measure-preserving Verlet integrators derived by Tuckerman et al.[8] Finally, we performed 10 ns of constant volume, constant temperature (NVT) dynamics at 298 K.

Radial distribution functions were obtained using the Visual Molecular Dynamics (VMD) software. Pictures of the various solvation shells, sampled from the simulation trajectory, where also obtained using VMD.

Quantum Chemistry Calculations

Quantum chemistry simulations were performed using the Q-Chem 5.1 quantum chemistry package[8]. Simulations involved a geometry optimization step at the B3LYP//6-31+G(d,p) level of theory followed by single point energy analysis at the B3LYP//6-311++G** level of theory. The HOMO orbitals and energy values were taken from the latter step. The orbital visualizations were produced in the Avogadro software using checkpoint files from the single point analysis.

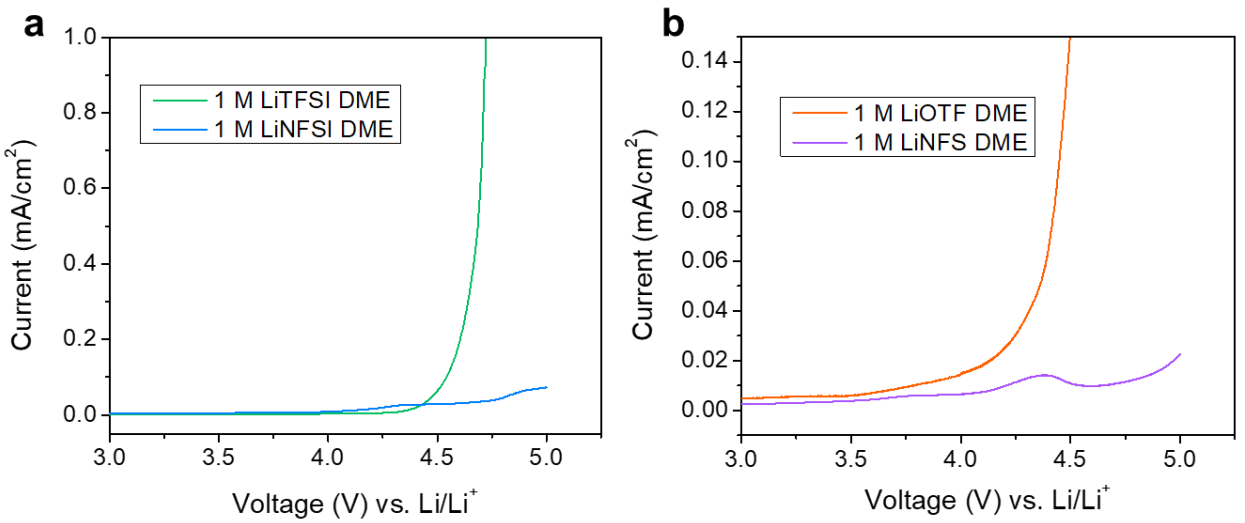

Figure S1. Linear-scan voltammetry of electrolytes of interest in Li||stainless steel coin cells at 1 mV s^{-1}. LSV profiles of cells utilizing **a)** 1 M LiTFSI and 1 M LiNFSI in DME, **b)** 1 M LiOTF and 1 M LiNFS in DME.

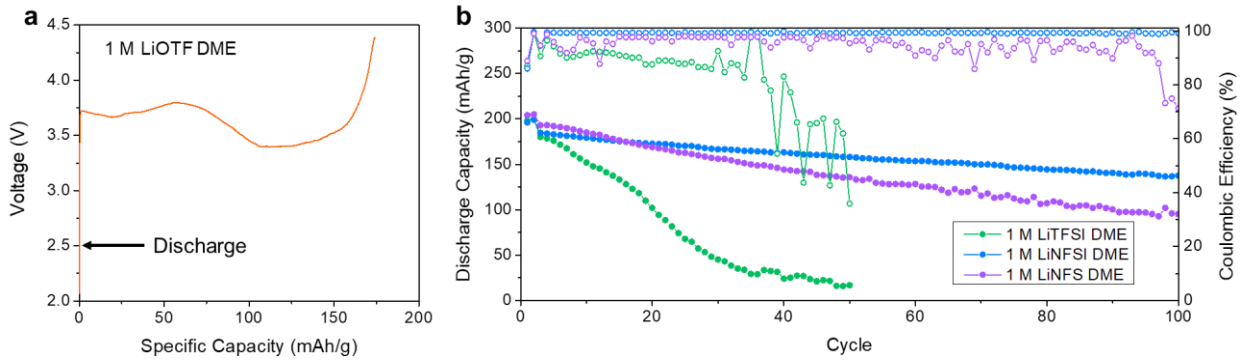

Figure S2. Galvanostatic cycling performance of Li||NMC 811 half cells using NMC 811 electrodes at an NMC 811 : Super P : PVDF mass ratio of 96:2:2. **a)** First cycle voltage profile of cells employing 1 M LiOTF DME, and **b)** extended cycling performance of cells employing 1 M LiTFSI, 1 M LiNFSI, and 1 M LiNFS DME.

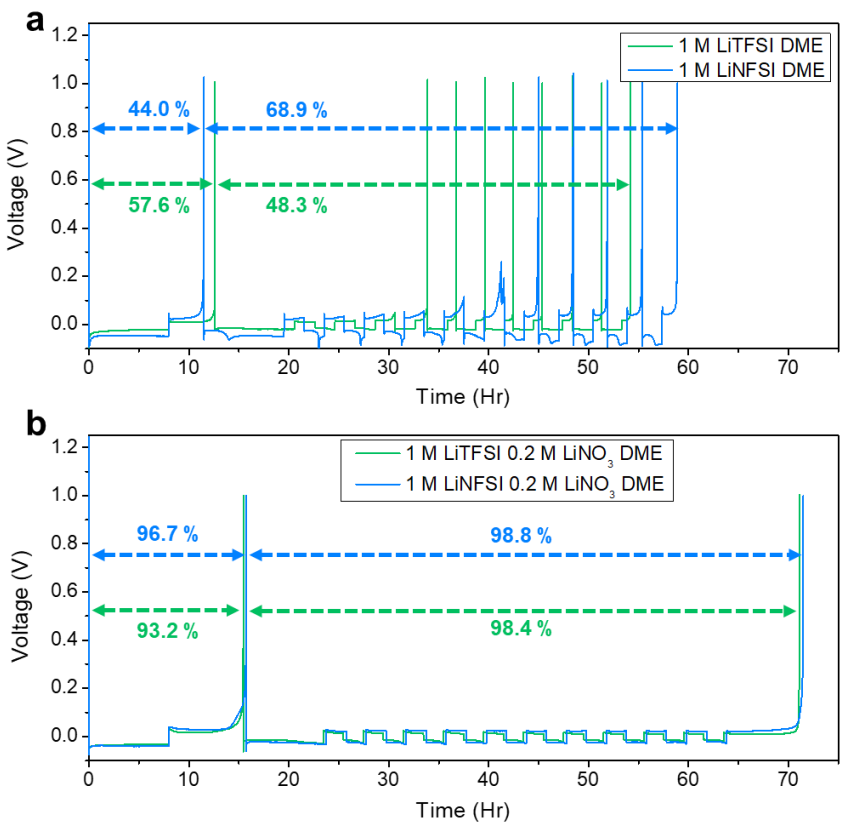

Figure S3. Li metal coulombic efficiency measurements in Li||Cu half cells employing LiTFSI and LiNFSI-based electrolytes. **a)** Profiles and corresponding CE values of 1 M LiTFSI DME and 1 M LiNFSI DME. **b)** Profiles and corresponding CE values of 1 M LiTFSI 0.2 M $LiNO_3$ DME and 1 M LiNFSI 0.2 M $LiNO_3$ DME.

Table S1. MD simulation details. Box volume and densities were determined from the equilibrated structures under 1 atm of isotropic pressure.

Electrolyte System	# Salt Molecules in Box	# DME Molecules in Box	Box Volume (nm^3)	System Density ($g\ mL^{-1}$)
1 M LiTFSI DME	20	255	49.7	0.960
1 M LiNFSI DME	20	255	55.7	1.036
1 M LiOTF DME	20	255	48.2	0.899
1 M LiNFS DME	20	255	51.3	0.942

Table S2. Comparison of HOMO energies from DFT simulations of anion/solvent pairs and individual electrolyte components in vacuum.

	HOMO (eV)		HOMO (eV)
$TFSI^-$ + DME	-8.28	$TFSI^-$	-8.41
$NFSI^-$ + DME	-8.55	$NFSI^-$	-9.17
OTF^- + DME	-7.88	OTF^-	-7.73
NFS^- + DME	-7.95	NFS^-	-8.04
		DME	-10.90

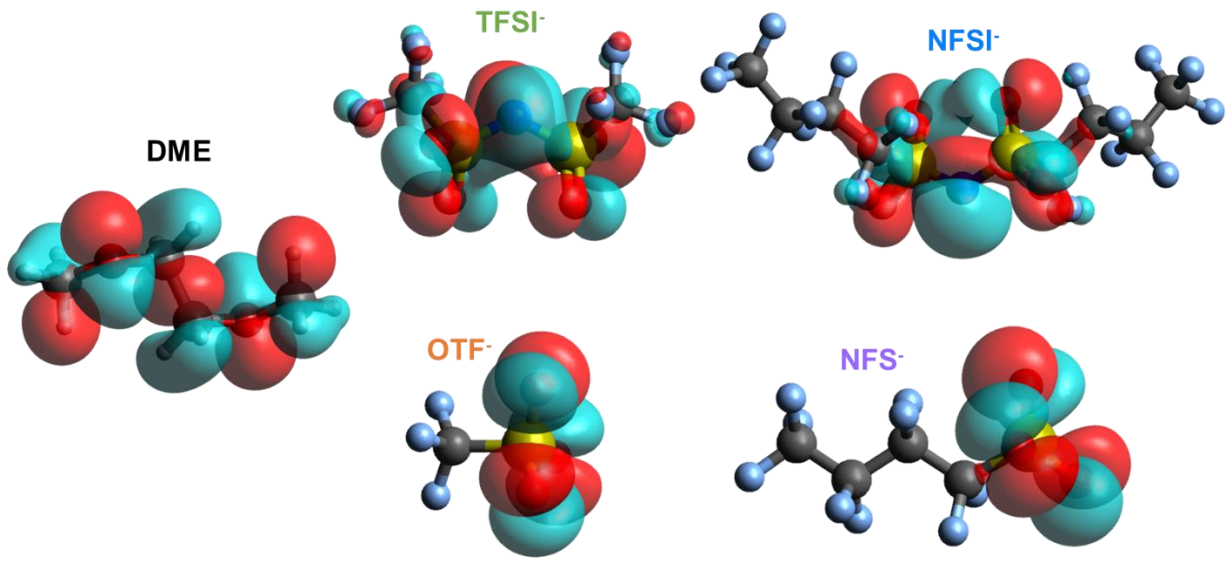

Figure S4. HOMO visualizations of individual electrolyte components from DFT calculations in vacuum.

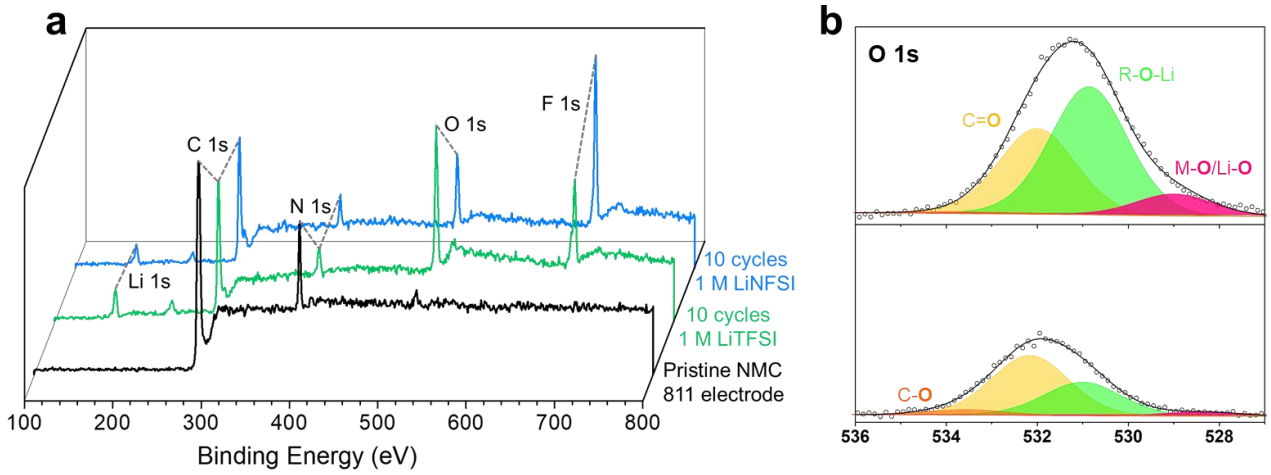

Figure S5. X ray photoelectron spectroscopy analysis of the CEI formed on NMC 811 electrodes employing a PAN binder after 10 cycles in 1 M LiTFSI DME and 1 M LiNFSI DME. **a)** Full XPS spectra of samples of interest compared with the pristine electrode, and **b)** O 1s spectra of the samples of interest.

References

[1] Adams, B. D.; Zheng, J.; Ren, X.; Xu, W.; Zhang, J.-G. Accurate Determination of Coulombic Efficiency for Lithium Metal Anodes and Lithium Metal Batteries. *Advanced Energy Materials 8* (7), 1702097.

[2] Kaminski, G. A.; Friesner, R. A.; Tirado-Rives, J.; Jorgensen, W. L. Evaluation and Reparametrization of the OPLS-AA Force Field for Proteins via Comparison with Accurate Quantum Chemical Calculations on Peptides. *J. Phys. Chem. B* **2001**, *105* (28), 6474–6487.

[3] L. Gouveia, A. S.; S. Bernardes, C. E.; C. Tomé, L.; I. Lozinskaya, E.; S. Vygodskii, Y.; S. Shaplov, A.; Canongia Lopes, J. N.; M. Marrucho, I. Ionic Liquids with Anions Based on Fluorosulfonyl Derivatives: From Asymmetrical Substitutions to a Consistent Force Field Model. *Physical Chemistry Chemical Physics* **2017**, *19* (43), 29617–29624.

[4] Park, C.; Kanduč, M.; Chudoba, R.; Ronneburg, A.; Risse, S.; Ballauff, M.; Dzubiella, J. Molecular Simulations of Electrolyte Structure and Dynamics in Lithium–Sulfur Battery Solvents. *Journal of Power Sources* **2018**, *373*, 70–78.

[5] W. Shinoda, M. Shiga, M. Mikami, Rapid estimation of elastic constants by molecular dynamics simulation under constant stress, Physical Review B 69 (2004) 134103.

[6] G.J. Martyna, D.J. Tobias, M.L. Klein, Constant pressure molecular dynamics algorithms, J. Chem. Phys. 101 (1994) 4177-4189.

[7] M. Parrinello, A. Rahman, Polymorphic transitions in single crystals: A new molecular dynamics method, J. Appl. Phys. 52 (1981) 7182-7190.

[8] M.E. Tuckerman, J. Alejandre, R. López-Rendón, A.L. Jochim, G.J. Martyna, A Liouville-operator derived measure-preserving integrator for molecular dynamics simulations in the isothermal–isobaric ensemble, J. Phys. A: Math. Gen. 39 (2006) 5629.

[9] Y. Shao, Z. Gan, E. Epifanovsky, A.T. Gilbert, M. Wormit, J. Kussmann, A.W. Lange, A. Behn, J. Deng, X. Feng, Advances in molecular quantum chemistry contained in the Q-Chem 4 program package, Mol Phys 113 (2015) 184-215.